

Magnetic OB[A] Stars with *TESS*: probing their Evolutionary and Rotational properties (MOBSTER) - I. First-light observations of known magnetic B and A stars

A. David-Uraz,¹★ C. Neiner,² J. Sikora,^{3,4} D. M. Bowman,⁵ V. Petit,¹ S. Chowdhury,⁶ G. Handler,⁶ M. Pergeorelis,¹ M. Cantiello,^{7,8} C. Erba,¹ Z. Keszthelyi,^{4,3} O. Kochukhov,⁹ J. Labadie-Bartz,¹⁰ R. MacInnis,¹ S. P. Owocki,¹ H. Pablo,¹¹ M. E. Shultz,¹ A. ud-Doula,¹² G. A. Wade,⁴ and the MOBSTER Collaboration

¹Department of Physics and Astronomy, University of Delaware, Newark, DE 19716, USA

²LESIA, Observatoire de Paris, PSL University, CNRS, Sorbonne Université, Univ. Paris Diderot, Sorbonne Paris Cité, 5 place Jules Janssen, F-92195 Meudon, France

³Department of Physics, Engineering Physics & Astronomy, Queen's University, Kingston, ON Canada, K7L 3N6

⁴Department of Physics and Space Physics, Royal Military College of Canada, PO Box 17000 Kingston, Ontario K7K 7B4, Canada

⁵Instituut voor Sterrenkunde, KU Leuven, Celestijnenlaan 200D, B-3001 Leuven, Belgium

⁶Nicolaus Copernicus Astronomical Center, Bartycka 18, 00-716 Warszawa, Poland

⁷Center for Computational Astrophysics, Flatiron Institute, 162 5th Avenue, New York, NY 10010, USA

⁸Department of Astrophysical Sciences, Princeton University, Princeton, NJ 08544, USA

⁹Department of Physics and Astronomy, Uppsala University, Box 516, 75120, Uppsala, Sweden

¹⁰Instituto de Astronomia, Geofísica e Ciências Atmosféricas, Universidade de São Paulo, Rua do Matão 1226, Cidade Universitária, 05508-900 São Paulo, SP, Brazil

¹¹AAVSO Headquarters, 49 Bay State Rd., Cambridge, MA, 02138, USA

¹²Penn State Scranton, 120 Ridge View Drive, Dunmore, PA 18512, USA

Accepted XXX. Received YYY; in original form 2019 March 8

ABSTRACT

In this first paper of a series, we introduce the MOBSTER collaboration (Magnetic OB[A] Stars with *TESS*: probing their Evolutionary and Rotational properties) and lay out its scientific goals. We present first results based on the analysis of the known magnetic O, B and A stars observed in 2-minute cadence in sectors 1 and 2 of the Transiting Exoplanet Survey Satellite (*TESS*) mission. We derive precise periods from the newly obtained light curves and compare them to previously published values. We also discuss the overall photometric phenomenology of the known magnetic massive and intermediate-mass stars and propose an observational strategy to augment this sample by taking advantage of the high-quality observations produced by *TESS*.

Key words: stars: early-type – stars: magnetic field – stars: rotation – techniques: photometric

1 INTRODUCTION

Unlike their lower-mass counterparts (e.g. Böhm-Vitense 2007), massive and intermediate-mass stars are not known to host contemporaneous, dynamo-generated magnetic fields at their surfaces. Instead, there exists a distinct population of magnetic O-, B- and A-type stars whose fields appear to be of fossil origin (Borra et al. 1982; Neiner et al. 2015; Alecian

et al. 2017). Despite the fact that this spectral type range covers a large variety of stellar parameters (masses, radii, luminosities), the incidence rate of detectable magnetic fields in these stars seems to be uniformly small, ~10% (Wade et al. 2014; Morel et al. 2015; Grunhut et al. 2017; Sikora et al. 2019). Magnetic OBA stars host strong fields that typically have large-scale, mostly dipolar topologies that are stable over decades (for a broader review, see e.g. Donati & Landstreet 2009).

These stars exhibit a range of phenomenologies that can be understood in terms of the interaction between their mag-

★ E-mail: adu@udel.edu

netic fields and their photospheres or atmospheres. In particular, since the magnetic field is not generally aligned with the rotational axis, many observables across the electromagnetic spectrum are found to be rotationally modulated, in a manner that is understood in the context of the Oblique Rotator Model (Stibbs 1950).

In earlier-type magnetic massive stars, the interaction between the magnetic field and the strong, supersonic line-driven stellar winds leads to the formation of a *magnetosphere* (ud-Doula & Owocki 2002), the detailed characteristics of which are determined by the stellar rotation rate, wind parameters and magnetic field strength (Townsend & Owocki 2005; ud-Doula et al. 2009; Petit et al. 2013). More specifically, *dynamical magnetospheres* (DMs) are formed around slow rotators and consist of outflowing ionized material channeled by the closed magnetic field lines, creating strong shocks near the magnetic equator and then once radiatively cooled, falling back onto the stellar surface in complex dynamic flows. Fast rotators additionally form a *centrifugal magnetosphere* (CM): centrifugal support prevents material from falling back onto the star, forming dense clouds which co-rotate with the stellar surface.

The presence of a magnetosphere around these massive stars is evidenced by observations at many different wavelengths. In the optical, periodic variations in H α are detected (e.g. Howarth et al. 2007; Bohlender & Monin 2011; Grunhut et al. 2012; Rivinius et al. 2013), as well as line profile variations in wind-sensitive resonance lines (primarily in the ultraviolet; e.g. Stahl et al. 1996; Marcolino et al. 2012), variable emission in the X-rays (Sanz-Forcada et al. 2004) and in the infrared (Oksala et al. 2015), and, in some cases, emission in the radio (e.g. Chandra et al. 2015; Kurapati et al. 2017; Leto et al. 2018). Some of these observations can be understood using magnetohydrodynamic (MHD) simulations of magnetospheres (e.g. ud-Doula et al. 2013; Marcolino et al. 2013; Nazé et al. 2014), as well as simplified analytical prescriptions such as the “Analytical Dynamical Magnetosphere” model for DMs (ADM; Owocki et al. 2016) and the “Rigidly Rotating Magnetosphere” model for CMs (RRM; Townsend & Owocki 2005).

In intermediate-mass stars, the effect of magnetism is somewhat different, as they do not possess the same fast, dense winds that higher mass stars do. Instead, fossil fields are known to affect diffusive processes in their radiative envelope (Michaud 1970; Alecian & Stift 2007), often leading to chemical abundance patches on their surface and, as a result, rotationally modulated peculiarities in their spectra (e.g. Kochukhov et al. 2015; Yakunin et al. 2015; Silvester et al. 2017). The energy distributions associated with magnetic intermediate-mass stars are also known to exhibit abnormal flux depressions in the UV (Kodaira 1969; Adelman 1975; Maitzen 1976). This is understood to be a direct consequence of the presence of strong surface magnetic fields (Kochukhov et al. 2005).

Of particular relevance to *TESS*, both massive and intermediate-mass stars with surface magnetic fields are known to exhibit periodic photometric variations associated with rotational modulation. In the case of earlier-type stars (earlier than about B1), these variations are due to a changing column density as the viewing angle through the magnetosphere varies with phase. This can be seen for stars with both DMs (e.g. HD 191612; Wade et al. 2011) and with

CMs (e.g. σ Ori E; Townsend 2008; Townsend et al. 2013). For later-type magnetic stars (later than about B5), photometric variations are associated to their surface chemical inhomogeneities, which also cause brightness spots. In fact, two classes of variable stars, as defined by the General Catalog of Variable Stars (GCVS; Samus’ et al. 2017), correspond to chemically peculiar B and A-type stars understood to host strong magnetic fields, respectively the SX Arietis and α^2 Canum Venaticorum (α^2 CVn) variables. Finally, for stars with an intermediate spectral type (roughly between B1 and B5), their photometric variability can be caused by either one of the two aforementioned effects, although it is often dominated by photospheric inhomogeneities. Indeed, even when magnetospheric eclipses are seen, there can still be a signature associated with chemical spots (as is the case with σ Ori E; Oksala et al. 2015). Furthermore, pulsations can also cause photometric variations in a subset of magnetic OBA stars, notably slowly-pulsating B stars (SPB; Waelkens & Rufener 1985), β Cephei variables (e.g. Struve 1952), δ Scuti pulsators (e.g. Fath 1937) and rapidly oscillating Ap (roAp) stars (Kurtz 1982).

Therefore, optical time-series photometry can be a powerful means of characterizing known magnetic OBA stars and identifying promising magnetic candidates. With the rise of high-precision space-based photometric missions over the last decade (e.g. *MOST*, CoRoT, *Kepler*, K2, BRITE-Constellation) and given its relatively much greater availability and time-sampling compared to high-resolution spectropolarimetry, we can leverage these observations to further our understanding of phenomena associated with stellar magnetism in the upper Hertzsprung-Russell Diagram (HRD). This could, for instance, provide evidence for the presence of magnetic fields in extra-Galactic Of?p stars (Nazé et al. 2015; Munoz et al. 2018), a spectral class known to be associated with magnetism in the Milky Way (Grunhut et al. 2017).

The Transiting Exoplanet Survey Satellite (*TESS*; Ricker et al. 2015) is the latest high-precision photometric space mission. During its two-year nominal mission time, it will observe 85 per cent of the full sky, in overlapping sectors of 96×24 deg, for a total of roughly 470 million point sources observed in full-frame images. The targets will be observed with various temporal baselines, from 27.4 d to almost 1 y, depending on their position on the sky. Designed to search for exoplanets transiting in front of their host star, *TESS* was launched on April 18, 2018, and started delivering public data of the first two observed 27.4-d sectors of the sky in December 2018. Given their high quality, these data can be used for a wide range of astronomical investigations in addition to exoplanet detections, including detailed asteroseismology and, in our case, studies of rotational modulation associated to stellar magnetism in early-type stars.

1.1 The MOBSTER collaboration

The MOBSTER collaboration (Magnetic OB[A] Stars with *TESS*: probing their Evolutionary and Rotational properties) aims to leverage *TESS* observations to gain further insight and understanding into the nature of magnetic massive and intermediate-mass stars. In particular, this project focuses on three types of targets:

- Known magnetic OBA stars with rotational periods shorter than ~ 27 d: these targets will be observed for at least one full rotational cycle during the *TESS* and their photometric variations can be used to test and calibrate analytical models by comparing them to synthetic light curves;
- Known magnetic OBA stars with a rotational period greater than ~ 27 d: these targets will likely be observed for only part of their rotational cycle, therefore shorter-term, potentially stochastic processes (e.g. dynamic flows in a DM) as well as other phenomena (such as pulsations) can be investigated; and
- New magnetic OBA candidates: we can identify magnetic candidates directly from their light curves and flag them for spectropolarimetric follow-up; such an observational strategy has proven highly successful for K2 data (Buyschaert et al. 2018). Such efforts are also led in parallel with similar studies classifying variability types in OBA stars observed by *TESS* (e.g. Pedersen et al. 2019; Balona et al. 2019, for the study of roAp stars using *TESS* data see Cunha et al. submitted).

High-quality light curves from *TESS* will allow us to pursue various science goals, such as the asteroseismic characterization of magnetic massive stars (which can teach us about the internal effects of surface magnetic fields; e.g. Briquet et al. 2012; Buyschaert et al. 2018) and precise determinations of their rotation periods. In this first paper of a series, we focus on the latter objective as we present newly-determined rotation periods for 16 known magnetic B and A stars¹ which were observed in *TESS* sectors 1 and 2² and compare them to previously published values.

In Section 2, we present the observations. In Section 3, we report results for known magnetic B and A stars, and discuss each star individually. Finally, we present our conclusions and consider future work in Section 4.

2 TESS OBSERVATIONS

The *TESS* data included and analyzed here are the 2-min light curves provided by the *TESS* Science Team and which are publicly available via the Mikulski Archive for Space Telescopes (MAST)³. A description of the data processing pipeline of these light curves is provided by Jenkins et al.

¹ By ‘known magnetic stars’, we designate stars whose surface magnetic fields have been directly detected with spectropolarimetry. The relevant references for each star’s magnetic detection can be found in section 3.2. According to that definition, no known magnetic O star was observed in sectors 1 and 2, while 4 magnetic B stars and 12 magnetic A stars were observed. 9 more B and A-type stars (HD 3988, HD 10840, HD 18610, HD 19400, HD 58448, HD 65950, HD 221507, HD 203932 and HD 221760) either yielded spurious or marginal detections in spectropolarimetric observations, or have magnetic field measurements which were obtained via other means (e.g. spectroscopy, without polarimetry), and were not included in this sample.

² While our sample comprises magnetic targets that were observed in sectors 1 and 2, a few of these stars (namely HD 53921, HD 24188 and HD 54118) were also observed in sector 3, so we included these data in our analysis.

³ <https://archive.stsci.edu/missions-and-data/transiting-exoplanet-survey-satellite-tess>

(2016). Full-frame images with 30-min cadence are not considered within the scope of this paper. Sector 1 was observed from July 25 to August 22, 2018, while sector 2 was observed from August 23 to September 20, 2018.

To select our sample, we cross-matched the list of observed stars in sectors 1 and 2 with the SIMBAD database (Wenger et al. 2000) and considered all the stars with known spectral types of A and earlier. We then used the same procedure as described by Pedersen et al. (2019) to perform a similar detrending by fitting and removing smooth, low-amplitude variations. The orbital period of *TESS* is 13.7 days and a gap is present in the data with this period (i.e. in the middle of a 27.4-d light-curve). There are also occasional instrumental artefacts (especially towards the end of the run in sector 1) which are addressed by performing 3σ clipping and removing any additional noisy data. To evaluate the point-to-point photometric precision of each light curve, we use the `ticgen` tool (Jaffe & Barclay 2017), a publicly distributed PYTHON package that allows users to query the *TESS* Input Catalog (TIC; Stassun et al. 2018). These values are included in Table 1.

Among the ~ 1150 OBA stars (excluding subdwarfs) available in *TESS* sectors 1 and 2, there are no known magnetic O star, four known magnetic B star, and twelve known magnetic A stars. Our detrended 2-min light curves of magnetic B and A stars observed in *TESS* sectors 1 and 2 are presented in Fig. 1 (B stars) and Fig. 2 (A stars). These sixteen objects are discussed below.

3 RESULTS

3.1 Photometric analysis

First, to measure accurate rotation periods using the *TESS* light curves, we improve the detrending of these light curves by manually removing obvious outliers and by fitting rotational modulation (when appropriate) assuming periodicity in the rotation frequency and its significant harmonics, following the technique detailed by Bowman et al. (2018). This allows us to both evaluate the rotation periods precisely and model and subtract the residuals (after having evaluated their scatter) using a locally weighted scatterplot smoothing (LoWeSS; Cleveland 1979; Seabold & Perktold 2010) filter, thus improving the long-term detrending.

Finally, we perform a Lomb-Scargle analysis (Lomb 1976; Scargle 1982) of these detrended light curves of our 16 targets by using the `LombScargle` class in the `astropy.stats` Python package. The results are presented in Figs. 1 and 2.

Out of our sixteen targets, thirteen show a clear peak in their periodogram that could be ascribed to rotation. Out of those, eleven show at least one harmonic of that frequency, the exceptions being CPD-60 944B and HD 218495. The amplitudes of the various signals that we detect are well within the typical range associated to α^2 CVn variables, with HD 65712 showing the greatest amplitude (nearly 60 mmag). We further detail our findings for individual stars in the following subsection.

Rotational periods are reported in Table 1. The uncer-

tainties are propagated using the following equation (from Bloomfield 1976 and Montgomery & Odonoghue 1999):

$$\sigma_f = \frac{\sqrt{6}\sigma_r}{\pi\sqrt{N}AT} \quad (1)$$

where σ_f and σ_r represent, respectively, the uncertainty on the measured frequency and the photometric uncertainty, N is the number of points in the light curve, A is the amplitude of the corresponding peak in the periodogram and T corresponds to the temporal baseline of the time series. In this case, using the photometric precision computed with `ticgen` might not fully account for the scatter that is present in the light curve, therefore we use the scatter of the residuals of the pre-whitened light curve after the multi-harmonic rotational model has been removed, as described above. In our results, we quote uncertainties in measured rotation periods as three times the formal uncertainty determined using Eq. 1, to account for the average difference in noise levels in the high and low frequency regimes (i.e. ‘pink noise’) often found in oversampled time-series data (see Schwarzenberg-Czerny 2003; Degroote et al. 2009; Holdsworth et al. 2018; Bowman et al. 2018).

Finally, the light curves of the stars for which a low-frequency peak potentially associated with rotation is recovered are phase folded using measured rotation periods and presented in the Appendix (Fig. A2).

3.2 Notes on individual stars

Most of the following stars have multiple period determinations in the literature, but whenever possible, we have reported the periods derived by Dubath et al. (2011) using Hipparcos photometry in Table 1 for consistency across the sample and to facilitate comparison. These periods are generally found to be reliable, except in a couple of cases (HD 203006, for which half of the rotational period is recovered, and HD 3980 for which the period is probably wrong).

HD 223640 (B9pSiSrCr, V = 5.18)

A photometric period of 3.73 ± 0.03 d was derived for HD 223640 (Morrison & Wolff 1971), a period that was also confirmed spectroscopically (Mégessier 1974, 1975), with infrared observations (Catalano et al. 1991, 1998b), and with variations of He I $\lambda 5876$ (that were however observed to be out of phase with the other reported variability; Catanzaro et al. 1999). The photometric period has been refined a number of times since (Kodaira 1973; North & Burnet 1991), and more recently to 3.735239 ± 0.000024 d using photometry and magnetic measurements (North et al. 1992). We measure a consistent period of 3.7349 ± 0.0005 d in the *TESS* data. Changes in the shape of the light curve over time have been proposed to be indicative of precession of the magnetic axis (Adelman & Knox 1994; Adelman 1997, 1999).

HD 223640 was first found to be magnetic by Babcock (1958), although its field was not detected in a more recent FORS1 spectropolarimetric observation (Hubrig et al. 2006; Bagnulo et al. 2015). This is not surprising as the observation was taken at the rotational phase corresponding

to a magnetic null in the field curve of North et al. (1992).

HD 53921 (B9III + B8V, V = 5.64)

Out of the sixteen known magnetic stars presented in this study, HD 53921 is the only one that is not known to exhibit chemical peculiarities in its spectrum. The Hipparcos photometry reveals a 1.65-d period which is attributed to a gravity pulsation mode making HD 53921 a slowly-pulsating B star (SPB) (Waelkens et al. 1998), and its radial velocity is also found to vary with the same period (1.6518 d; Aerts et al. 1999). However, lower frequencies were also detected in the radial velocity measurements, possibly indicating long-period orbital variations (De Cat et al. 2000; consistent with a visual double with separation > 1 arcsec, e.g. Horch et al. 2001). This scenario was confirmed by De Cat & Aerts (2002), who found HD 53921 to be an eccentric SB1 with a period of ~ 340 d. The components have a ~ 1 magnitude difference in the *V* band, with the brightest having a spectral type of B9III, and the fainter one B8V (Corbally 1984).

The photometric variations are difficult to reconcile with non-radial pulsations (Townsend 2002) and mode identification has proven to be arduous (De Cat et al. 2005). Its pulsational frequency lies within the (large) range of possible rotational frequencies based on its projected rotational velocity and inferred radius (Szewczuk & Daszyńska-Daszkiewicz 2015).

Claimed to be magnetic despite what appears to be a marginal detection by Hubrig et al. (2006), it was however confirmed to be magnetic by Bagnulo et al. (2012). Bagnulo et al. (2015) later identified the B9III primary as the magnetic star. The published SPB frequency is recovered in the *TESS* data (1.65183 ± 0.00002 d). Further magnetic characterization would help clarify the nature of this frequency and determine the rotational period of the primary.

CPD-60 944B (B9pSi, V = 8.76)

CPD-60 944B is a member of a $\sim 10''$ visual pair within the open cluster NGC 2516 (Snowden 1975). Its visual companion, CPD-60 944A, might be itself a binary (González & Lapasset 2000), a hypothesis that has also been supported by González et al. (2014), who propose an orbital period of 121.6 d or 182.5 d (they also propose CPD-60 944B to be a HgMn star, something that is not supported by other studies). There has historically been some degree of confusion between both of these stars, and the membership of CPD-60 944B in NGC 2516 has been questioned (e.g. Frinchaboy & Majewski 2008).

Bernhard et al. (2015) measured a photometric period of 3.7367 ± 0.0003 d and attributed it to component A, although both visual components were within the aperture of ASAS-3. We report this period in Table 1, since we find a similar period in the *TESS* observations (3.759 ± 0.002). However both visual components also fall within the *TESS* aperture. The difference between both values could be attributable to aliasing. A marginal magnetic field detection was reported by Bagnulo et al. (2006), and later confirmed by Bagnulo et al. (2015).

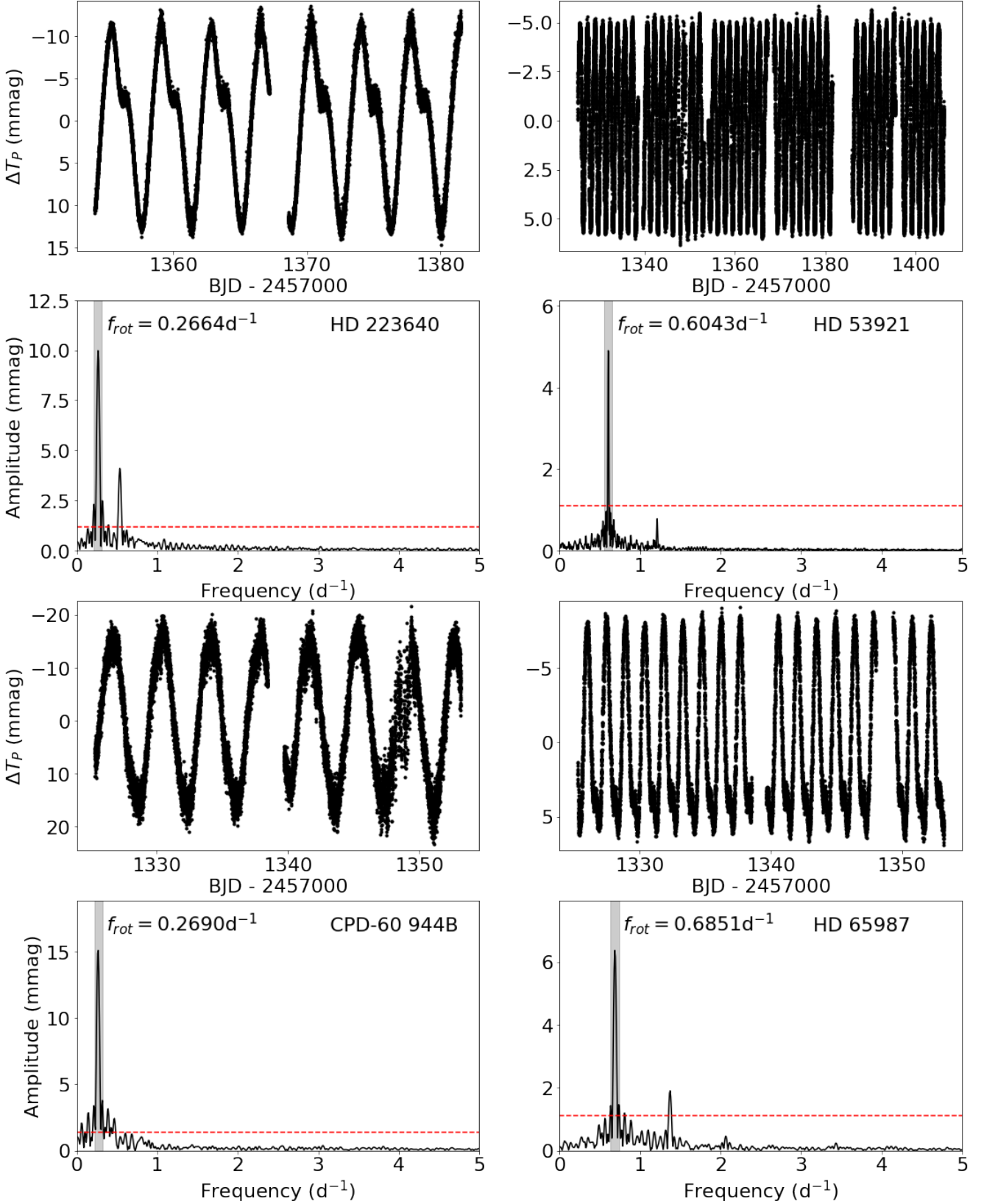


Figure 1. Light curves and Lomb Scargle periodograms for each of the four known magnetic B stars observed by *TESS* in its sectors 1 and 2. The inferred rotational frequency for each star is highlighted and labelled. In each periodogram, the horizontal dashed red line corresponds to three times the point-to-point photometric precision (as listed in Table 1, and converted to mmag) to indicate roughly the significance of a peak in the amplitude spectrum prior to removal via pre-whitening.

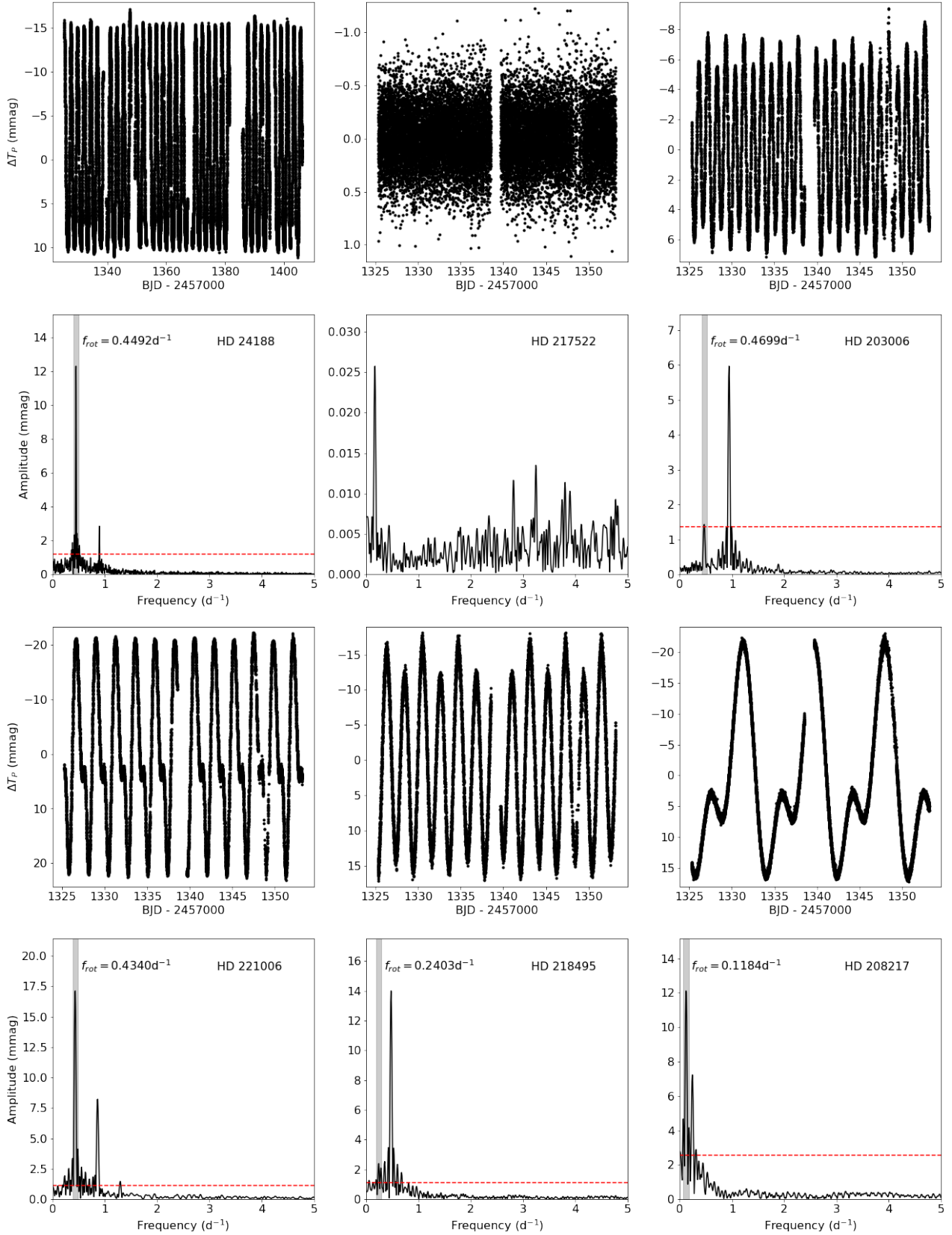


Figure 2. Same as Fig. 1, but for the A stars. For some periodograms, for example HD 217522's, no horizontal dashed red line is shown since it actually lies above the plotted range, which coupled with the lack of at least an additional significant harmonic (except perhaps in the case of HD 66318) casts doubt on the interpretation of rotational modulation as the cause of the low-amplitude peaks in these stars.

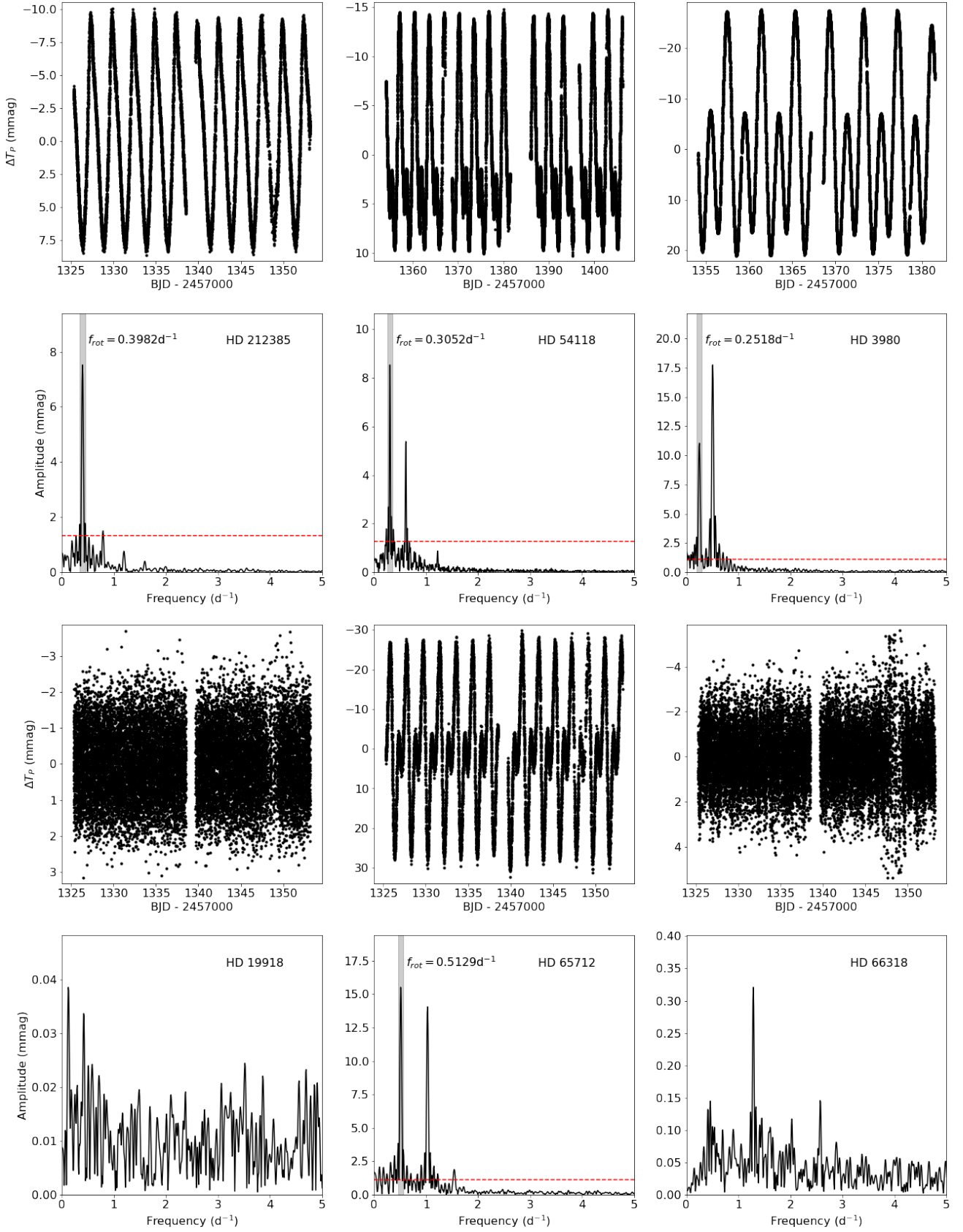


Figure 3. Continued

Table 1. List of known magnetic B- and A-type stars observed by *TESS* in sectors 1 and 2. For each star, we provide the TIC number, a more common identifier (mostly the HD number), the spectral type, the *TESS* instrumental magnitude and associated point-to-point photometric scatter, and three periods that are measured for the star (and that are long enough to potentially be associated with rotation, although in some cases they may be related to other phenomena such as pulsations): published periods based, respectively, on photometry and on other measurements, and our new refined periods derived from the *TESS* data. For these periods, the number appearing between parentheses corresponds to the uncertainty on the final digit of the reported period; the absence of such a number denotes an unreported uncertainty. Finally, we report the largest measured longitudinal magnetic field for each star (and its uncertainty) and the total number of spectropolarimetric observations referenced in the literature (an asterisk denotes a star for which these measurements are considered to be phase resolved, while a question mark indicates a lower limit, provided that some sources did not clearly state the total number of observations).

TIC no.	Name	Sp. type	Tmag	Scatter (ppm)	Phot. period (d)	Other period (d)	<i>TESS</i> period (d)	$ B_{z, \max} $ (G)	N_s
89545031	HD 223640	B9pSiSrCr ^a	5.32	340	3.7342 ^c	3.735239(24) ^j	3.7349(5)	1390±220	40*
279511712	HD 53921	B9III+B8V ^b	5.80	347	1.6520 ^c	1.6518 ^k	1.65183(2)	511±83	5
358467049	CPD-60 944B	B9pSi ^a	8.74	654	3.7367(3) ^d	N/A	3.759(2)	463±72	2
372913684	HD 65987	B9pSiSr ^a	7.65	466	1.44962(18) ^e	~ 9 ^l	1.4561(1)	738±122	2
32035258	HD 24188	A0pSi ^a	6.42	368	2.2300 ^c	N/A	2.23024(4)	538±44	1
139191168	HD 217522	A5pSrEuCr ^a	7.17	417	N/A	N/A	N/A	1123±82	97
159834975	HD 203006	A2pCrEuSr ^a	4.90	338	1.0610 ^c	2.1219 ^m	2.143(3)	650±147	14
235007556	HD 221006	A0pSi ^a	5.82	348	2.3147 ^c	2.31483(40) ⁿ	2.3119(1)	990±180	3
237336864	HD 218495	A2pEuSr ^a	9.23	790	4.2006(1) ^f	N/A	4.183(6)	1169±56	5
277688819	HD 208217	A0pSrEuCr ^a	7.09	410	8.44475(11) ^g	8.44475(11) ^g	8.317(1)	1843±214	20?*
278804454	HD 212385	A3pSrEuCr ^a	6.78	388	2.5265(15) ^h	N/A	2.5062(2)	639±40	2
279573219	HD 54118	A0pSi ^a	5.30	340	3.2749 ^c	3.27533(20) ^o	3.2759(2)	1680±120	15*
281668790	HD 3980	A7pSrEuCr ^a	5.70	345	1.1628 ^c	3.9516(3) ^p	3.997(3)	1688±29	5
348717688	HD 19918	A5pSrEuCr ^a	9.12	756	N/A	N/A	N/A	777±109	2?
358467700	HD 65712	A0pSiCr ^a	9.30	813	1.943(1) ⁱ	N/A	1.94601(20)	1296±71	2
410451752	HD 66318	A0pEuCrSr ^a	9.56	908	N/A	N/A	N/A?	6480±91	2

References for the spectral types and published periods are the following: *a*) Renson & Manfroid (2009); *b*) Corbally (1984); *c*) Dubath et al. (2011); *d*) Bernhard et al. (2015); *e*) North (1984); *f*) Cunha et al. (submitted); *g*) Manfroid & Mathys (1997); *h*) Manfroid & Mathys (1985); *i*) Warhurst (2004); *j*) North et al. (1992); *k*) Aerts et al. (1999); *l*) Abt & Levy (1972); *m*) Maitzen et al. (1974); *n*) Leone et al. (1995); *o*) Bohlender et al. (1993); and *p*) Maitzen et al. (1980).

HD 65987 (B9pSiSr, V = 7.59)

HD 65987 was proposed to be an eclipsing binary system (Snowden 1975), and has often been classified as an eclipsing Algol variable (e.g. Avvakumova et al. 2013). Based on radial velocity measurements, Abt & Levy (1972) find a possible periodicity of ~9 d that could be associated to binarity. Avvakumova & Malkov (2014) evaluate the evolutionary status of this system to be a detached main sequence binary, based on its well-established membership in the NGC 2615 cluster (e.g. Landstreet et al. 2007).

Low-level photometric variability was first detected with a putative 1.41-d period (North et al. 1982), which was later refined to 1.44962 ± 0.00018 d by North (1984). If this value is assumed to be related to rotation, a small value of $R \sin i$ (Hensberge et al. 1991) would indicate that i is likely small. The *TESS* period (1.4561 ± 0.0001 d) is similar that of North (1984), and the data are of much better quality than the phased Hipparcos photometry presented by Heck et al. (1987). The difference between both periods appears to be due to annual aliasing. While we ascribe this period to rotation, a binary origin to the light curve variations is not conclusively ruled out. Interestingly, a small peak appears in the periodogram of the non-detrended light curve at a period of about 9 days, corroborating the idea that that period might be linked to binarity.

HD 65987 was found to be magnetic by Bagnulo et al. (2006), and that detection was later confirmed by Bagnulo

et al. (2015). However, new magnetic measurements with improved phase coverage do not seem to vary according to the photometric period (Landstreet et al. in prep.), making this system harder to interpret. More work will be required to confirm the origin of HD 65987's photometric variability.

HD 24188 (A0pSi, V = 6.26)

HD 24188 was found to exhibit non-linear proper motion, making it an astrometric binary candidate (Makarov & Kaplan 2005; Frankowski et al. 2007) even though it is not observed to be a spectroscopic binary (Grenier et al. 1999). Hipparcos photometry revealed a clear periodicity (2.230 d; Paunzen & Maitzen 1998), which they associated with rotation. We confirm this period in the *TESS* light curve (2.23024 ± 0.00004 d).

Based on a single spectropolarimetric observation, HD 24188 was found to be magnetic by Kochukhov & Bagnulo (2006), a conclusion which was since supported through the reanalysis of the same observation (Hubrig et al. 2006; Bagnulo et al. 2015).

HD 217522 (A5pSrEuCr, V = 7.52)

HD 217522 is a well-studied roAp star (13.72-min pulsational period; Kurtz 1983). It is one of the few roAp stars for which mode switching has been observed (Kreidl et al. 1991). However, no sign has been found of rotational mod-

ulation of the pulsational amplitudes (van Heerden et al. 2012), hence either the stellar surface is not very spotted or the rotational axis is nearly aligned with our line of sight, not allowing us to see rotational modulation, a hypothesis further supported by the very low measured value of $v \sin i$ (3 km s^{-1} ; Medupe et al. 2015). While the amplitude modulation occurs on short timescales ($\sim 1 \text{ d}$), it appears to be stochastic, similar to solar-type oscillations. This also appears to be qualitatively consistent with the fact that we do not find a significant low-frequency series of harmonics in the *TESS* observations of HD 217522, and in particular, no sign of rotation. Analysis of the high frequency variability using *TESS* observations is performed by Cunha et al. (submitted).

A marginal detection of a magnetic field was reported by Mathys & Hubrig (1997), and has since then been confirmed (Hubrig et al. 2004; Bagnulo et al. 2015). The field strength is not found to vary on the pulsational timescale (Hubrig et al. 2004; they acquired 91 short observations within $< 0.25 \text{ d}$, a time span insufficient to detect rotational modulation).

HD 203006 (*A2pCrEuSr*, $V = 4.82$)

HD 203006 is a visual double with a close faint companion (2 mag fainter in the Hipparcos bandpass, separation of $0.1''$, Lindegren et al. 1997). A number of rotation periods have been published for HD 203006. Morrison & Wolff (1971) first reported probable photometric periods of 0.941 d and 1.062 d , then it was refined to 1.0609 d by Maitzen (1973). It was realized that the rotation period was in fact about twice the previously published periods (2.1219 d , based on photometric and spectroscopic data; Maitzen et al. 1974), which was then refined to $2.1215 \pm 0.0001 \text{ d}$ (Deul & van Genderen 1983). We find a similar period in the *TESS* data ($2.143 \pm 0.003 \text{ d}$); it should be noted that it is not the strongest peak in the periodogram, as the first harmonic dominates the spectrum. The difference between the periods might be due to aliasing.

HD 203006 has also been observed to vary in the ultraviolet, although there were not enough observations to establish a period (van Dijk et al. 1978). Low-level variability was also observed in the near infrared with period of 2.1224 d (Catalano et al. 1998a). It was first observed to be magnetic by Babcock (1958). Later undetected by Borra & Landstreet (1980), its field was eventually confirmed by Bohlender & Landstreet (1990).

HD 221006 (*A0pSi*, $V = 5.68$)

HD 221006 was shown to vary photometrically with a period of $2.32 \pm 0.03 \text{ d}$ (Renson 1978), which was later refined to $2.3148 \pm 0.0004 \text{ d}$ (Manfroid & Mathys 1985). Spectroscopic variations also phase coherently with this period, as well as photometric variability in many filters, including in the infrared (Leone et al. 1995). The *TESS* photometry of HD 221006 shows a similar period of $2.3119 \pm 0.0001 \text{ d}$. This star was detected to be magnetic by Bohlender et al. (1993).

HD 218495 (*A2pEuSr*, $V = 9.38$)

HD 218495 was found to host high frequency pulsations

($P = 7.44 \text{ min}$; Martinez & Kurtz 1990; Martinez et al. 1991). No other variability period is reported in the literature for this roAp star prior to the *TESS* observations. Although the periodogram is clearly dominated by the first harmonic (see Fig. 2, the amplitude of the signal is clearly modulated on a period that is twice as long as the one that we would derive from the dominant peak), we determine a rotational period of $4.183 \pm 0.006 \text{ d}$. This is similar to the value given by Cunha et al. (submitted), which offer the first determination of this star's rotational period ($4.2006 \pm 0.0001 \text{ d}$).

A first attempt to observe HD 218495's magnetic field did not yield a significant detection (Mathys & Hubrig 1997), but it has since been found to be magnetic (Hubrig et al. 2004), a detection that was confirmed by Bagnulo et al. (2015).

HD 208217 (*A0pSrEuCr*, $V = 7.19$)

HD 208217 is an astrometric binary candidate based on proper motion measurements (Frankowski et al. 2007). HD 208217 was found to vary photometrically with a period of $8.35 \pm 0.10 \text{ d}$ (Manfroid & Renson 1983). Its period was refined to $8.44475 \pm 0.00011 \text{ d}$ (Manfroid & Mathys 1997) using both photometry and magnetic field modulus measurements derived from line broadening (for the latter see also Mathys et al. 1997; they mention this is a spectroscopic binary with a potentially long period, on the order of 2 years). We recover a slightly shorter period based on its *TESS* light curve ($8.317 \pm 0.001 \text{ d}$). The difference could be due to aliasing.

HD 208217's magnetic field was detected and measured to provide a phase-resolved longitudinal field curve by Landstreet & Mathys (2000), with additional follow-up measurements by Mathys (2017).

HD 212385 (*A3pSrEuCr*, $V = 6.84$)

HD 212385 exhibits non-linear proper motion which makes it an astrometric binary candidate (Makarov & Kaplan 2005; Frankowski et al. 2007). A period of $2.48 \pm 0.04 \text{ d}$ was found in photometry (Renson 1978), and then refined to $2.5265 \pm 0.0015 \text{ d}$ (Manfroid & Mathys 1985). We find a slightly shorter period in the *TESS* data ($2.5062 \pm 0.0002 \text{ d}$). The difference is likely due to yearly aliasing. HD 212385 was discovered to be magnetic by Hubrig et al. (2006), a detection confirmed by Kochukhov & Bagnulo (2006) and Bagnulo et al. (2015).

HD 54118 (*A0pSi*, $V = 5.17$)

Identified as an astrometric binary candidate due to non-linear proper motion (Makarov & Kaplan 2005; Frankowski et al. 2007), HD 54118 was later found to be a spectroscopic binary by Ammler-von Eiff & Reiners (2012), though its companion is not well characterized. Its optical light curve was found to vary on a period of $3.275 \pm 0.015 \text{ d}$ (Manfroid & Renson 1981), a period which was refined a few times (Manfroid & Mathys 1985; Catalano & Leone 1993), most recently to $3.27535 \pm 0.00010 \text{ d}$ (Manfroid & Renson 1994).

Found to be magnetic with $P_{\text{rot}} = 3.2 \pm 0.1 \text{ d}$ (Borra & Landstreet 1975), its field detection was confirmed by

Bohlender et al. (1993) using phase resolved observations; they also refined the period to 3.27533 ± 0.00020 d, which is consistent with the photometric period. There was also a further follow-up spectroscopic observation by Donati et al. (1997). The *TESS* light curve reveals a period of 3.2759 ± 0.0002 d, consistent with the previous results.

HD 3980 (A7pSrEuCr, V = 5.70)

HD 3980 is a known visual double (Kopal 1955; De Rosa et al. 2014; its companion is 2.89 mag fainter in the *K* band and separated by $\sim 13''$). The first photometric period determined for HD 3980 was 0.4 d (Maitzen 1976). Since then, different photometric periods have been reported: 2.13 d or 0.68 d (Renson 1979), and later 3.9516 ± 0.0003 d (Maitzen et al. 1980). The latter study also took into account magnetic measurements based on Zeeman line broadening/splitting. Photometric variability in the infrared (*J*, *H* and *K* bands) is also found to phase coherently with the optical period (Catalano et al. 1991, 1998a).

We find a slightly longer period in the *TESS* light curve (3.997 ± 0.003 d); it should be noted that it is not the strongest peak in the periodogram, as the first harmonic dominates the spectrum. The difference between both periods is probably due to yearly aliasing. Furthermore, the previous photometric period listed in Table 1 uses the automated determination made by Dubath et al. (2011); but that value is not found in our periodogram. The detection of a magnetic field at the surface of HD 3980 has been reported by Hubrig et al. (2006) and Bagnulo et al. (2015), supporting the earlier Zeeman line broadening measurements.

HD 19918 (A5pSrEuCr, V = 9.35)

HD 19918 is a well-known roAp star discovered in the Cape survey (Martinez & Kurtz 1991, 1994; Martinez et al. 1995; see also Cunha et al. submitted) with no visual companion (Schöller et al. 2012). A marginal field detection (Mathys & Hubrig 1997) was later confirmed by Kochukhov & Bagnulo (2006) (also see Hubrig et al. 2006; Bagnulo et al. 2015), and investigated through line broadening as well (Ryabchikova et al. 2007). No significant detection of a period on a rotational timescale is found in the *TESS* photometry.

HD 65712 (A0pSiCr, V = 9.35)

HD 65712 is a member of NGC 2516 (Snowden 1975), despite being identified as a possible high-velocity star by Jaschek et al. (1983). Its membership in the cluster was confirmed by Landstreet et al. (2007).

HD 65712 was found to have a 1.943 ± 0.001 -d photometric rotation period by Warhurst (2004), which was refined to 1.88 d by Paunzen et al. (2011). We find a period in the *TESS* photometry of this star (1.94601 ± 0.0002 d) that appears to be more consistent with the earlier determination of Warhurst (2004); hence, we choose to report that value in Table 1. A magnetic field was detected by Bagnulo et al. (2006) (and confirmed by Bagnulo et al. 2015).

HD 66318 (A0pEuCrSr, V = 9.56)

HD 66318 is a probable member of NGC 2516 (Cox 1955; Frinchaboy & Majewski 2008). This star has consistently been found to be photometrically constant (North et al. 1982; North 1987; Dachs & Kabus 1989). A strong magnetic field was detected by Bagnulo et al. (2003) and later confirmed by Bagnulo et al. (2006) and Bernhard et al. (2015), with a significant discrepancy observed between the field strengths measured from hydrogen and metal lines (Landstreet et al. 2014). These authors do not find spectral variability, suggesting a very long rotation period (potentially on the order of years). This is also consistent with their finding that the projected rotational velocity is very low as determined from high-resolution UVES spectra, contradicting previous findings that $v \sin i = 30 \text{ km s}^{-1}$ (Dachs 1972; Wolff 1981).

Similarly, we do not detect a significant period in the *TESS* photometry; as such, we reiterate the conclusion of Mathys (2017) that more observations are required to characterize the long-term variability of this star. However, there appears to be a potential rotational peak at 1.3 d^{-1} (and its first harmonic), hence the question mark in Table 1; given that the pixels from which this star's signal is measured are highly contaminated (contamination ratio of 0.815 according to the TIC), it is plausible that the flux of nearby stars is within the light curves of HD 66318. A similar conclusion is reached by Cunha et al. (submitted).

4 DISCUSSION AND CONCLUSIONS

Eleven out of the sixteen known magnetic B and A stars observed in the first two sectors of *TESS* show periodograms typical of rotation with a main frequency peak and at least one harmonic (although in at least one case the measured peak could instead be associated with SPB pulsations). This is a characteristic signature of rotational modulation, understood to be due to the presence of an oblique dipolar magnetic field. Other targets showing this behaviour in the periodogram of their *TESS* light-curves should be considered as promising magnetic candidates. Such candidates in sectors 1 and 2 have been identified for OB stars by Pedersen et al. (2019) and for A stars by Sikora et al. (in prep.). They are prime targets for future spectropolarimetric observations.

We have refined the period determinations for thirteen targets, and in some cases, compared to published values based both on photometric studies and other types of observations. We find our results to be consistent with the literature values overall, although in the case of six stars (CPD-60 944B, HD 65987, HD 203006, HD 208217, HD 212385 and HD 3980) it appears likely that aliasing caused systematic differences between them. These results also illustrate the immense potential of *TESS*, compared to other space-based large surveys, as we detect rotational modulation in three stars (HD 65987, HD 208217 and HD 212385) that were observed by Hipparcos, but for which no period was recovered. We also present phase folded light curves for these thirteen stars in the Appendix (Fig. A2); these show a wide variety of morphologies and nicely illustrate the exquisite quality of the *TESS* observations.

As for the three stars that did not show significant

low frequency peaks in their periodograms (HD 217522, HD 19918 and HD 66318), we are not able to conclude anything about their rotation periods. The first two stars are known to exhibit rapid oscillations, identifying them as roAp stars, while the last one is likely too heavily contaminated for its rotational modulation to be significantly detected (although a weak signal with a period of about 0.8 d might be present). The most useful constraint to evaluate these stars' rotation periods would be to obtain phase-resolved magnetic measurements.

Importantly, this paper also introduces the MOBSTER collaboration, a group consisting of both observers and theorists with the aim of using *TESS* data to further the study and characterization of magnetic OBA stars and to discover new magnetic stars out of a photometrically pre-selected sample of targets. Upcoming studies will include the characterization of specific objects of interest and confronting analytic models to observations.

ACKNOWLEDGEMENTS

This paper includes data collected by the *TESS* mission. Funding for the *TESS* mission is provided by the NASA Explorer Program. Funding for the *TESS* Asteroseismic Science Operations Centre is provided by the Danish National Research Foundation (Grant agreement no.: DNRFF106), ESA PRODEX (PEA 4000119301) and Stellar Astrophysics Centre (SAC) at Aarhus University. We thank the *TESS* and TASC/TASOC teams for their support of the present work. This research has made use of the SIMBAD database, operated at CDS, Strasbourg, France. Some of the data presented in this paper were obtained from the Mikulski Archive for Space Telescopes (MAST). STScI is operated by the Association of Universities for Research in Astronomy, Inc., under NASA contract NAS5-2655.

The authors are grateful to C.L. Fletcher for her linguistic assistance.

ADU acknowledges the support of the Natural Science and Engineering Research Council of Canada (NSERC). The research leading to these results received funding from the European Research Council (ERC) under the European Union's Horizon 2020 research and innovation program (grant agreement No. 670519: MAMSIE). JL-B acknowledges support from FAPESP (grant 2017/23731-1). AuD acknowledges support from NASA through Chandra Award number TM7-18001X issued by the Chandra X-ray Observatory Center, which is operated by the Smithsonian Astrophysical Observatory for and on behalf of NASA under contract NAS8-03060.

REFERENCES

Abt H. A., Levy S. G., 1972, *ApJ*, 172, 355
 Adelman S. J., 1975, *ApJ*, 195, 397
 Adelman S. J., 1997, *A&AS*, 125, 65
 Adelman S. J., 1999, *Baltic Astronomy*, 8, 369
 Adelman S. J., Knox Jr. J. R., 1994, *A&AS*, 103, 1
 Aerts C. et al., 1999, *A&A*, 343, 872
 Alecian E., Villebrun F., Grunhut J., Hussain G., Neiner C., Wade G. A., 2017, arXiv e-prints
 Alecian G., Stift M. J., 2007, *A&A*, 475, 659

Ammler-von Eiff M., Reiners A., 2012, *A&A*, 542, A116
 Avvakumova E. A., Malkov O. Y., 2014, *MNRAS*, 444, 1982
 Avvakumova E. A., Malkov O. Y., Kniazev A. Y., 2013, *Astronomische Nachrichten*, 334, 860
 Babcock H. W., 1958, *ApJS*, 3, 141
 Bagnulo S., Fossati L., Landstreet J. D., Izzo C., 2015, *A&A*, 583, A115
 Bagnulo S., Landstreet J. D., Fossati L., Kochukhov O., 2012, *A&A*, 538, A129
 Bagnulo S., Landstreet J. D., Lo Curto G., Szeifert T., Wade G. A., 2003, *A&A*, 403, 645
 Bagnulo S., Landstreet J. D., Mason E., Andretta V., Silaj J., Wade G. A., 2006, *A&A*, 450, 777
 Balona L. A. et al., 2019, arXiv e-prints
 Bernhard K., Hümmerich S., Otero S., Paunzen E., 2015, *A&A*, 581, A138
 Bloomfield P., 1976, *Fourier analysis of time series: an introduction*
 Bohlender D. A., Landstreet J. D., 1990, *MNRAS*, 247, 606
 Bohlender D. A., Landstreet J. D., Thompson I. B., 1993, *A&A*, 269, 355
 Bohlender D. A., Monin D., 2011, *AJ*, 141, 169
 Böhm-Vitense E., 2007, *ApJ*, 657, 486
 Borra E. F., Landstreet J. D., 1975, *PASP*, 87, 961
 Borra E. F., Landstreet J. D., 1980, *ApJS*, 42, 421
 Borra E. F., Landstreet J. D., Mestel L., 1982, *ARA&A*, 20, 191
 Bowman D. M., Buysschaert B., Neiner C., Pápics P. I., Oksala M. E., Aerts C., 2018, *A&A*, 616, A77
 Briquet M. et al., 2012, *MNRAS*, 427, 483
 Buysschaert B., Aerts C., Bowman D. M., Johnston C., Van Reeth T., Pedersen M. G., Mathis S., Neiner C., 2018, *A&A*, 616, A148
 Buysschaert B., Neiner C., Martin A. J., Aerts C., Bowman D. M., Oksala M. E., Van Reeth T., 2018, *MNRAS*, 478, 2777
 Catalano F. A., Kroll R., Leone F., 1991, *A&A*, 248, 179
 Catalano F. A., Leone F., 1993, *A&AS*, 97, 501
 Catalano F. A., Leone F., Kroll R., 1998a, *A&AS*, 129, 463
 Catalano F. A., Leone F., Kroll R., 1998b, *A&AS*, 131, 63
 Catanzaro G., Leone F., Catalano F. A., 1999, *A&AS*, 134, 211
 Chandra P. et al., 2015, *MNRAS*, 452, 1245
 Cleveland W. S., 1979, *Journal of the American Statistical Association*, 74, 829
 Corbally C. J., 1984, *ApJS*, 55, 657
 Cox A. N., 1955, *ApJ*, 121, 628
 Dachs J., 1972, *A&A*, 21, 373
 Dachs J., Kabus H., 1989, *A&AS*, 78, 25
 De Cat P., Aerts C., 2002, *A&A*, 393, 965
 De Cat P., Aerts C., De Ridder J., Kolenberg K., Meeus G., Decin L., 2000, *A&A*, 355, 1015
 De Cat P., Briquet M., Daszyńska-Daszkiewicz J., Dupret M. A., De Ridder J., Scuflaire R., Aerts C., 2005, *A&A*, 432, 1013
 De Rosa R. J. et al., 2014, *MNRAS*, 437, 1216
 Degroote P. et al., 2009, *A&A*, 506, 111
 Deul E. R., van Genderen A. M., 1983, *A&A*, 118, 289
 Donati J.-F., Landstreet J. D., 2009, *ARA&A*, 47, 333
 Donati J.-F., Semel M., Carter B. D., Rees D. E., Collier Cameron A., 1997, *MNRAS*, 291, 658
 Dubath P. et al., 2011, *MNRAS*, 414, 2602
 Fath E. A., 1937, *Lick Observatory Bulletin*, 487, 77
 Frankowski A., Jancart S., Jorissen A., 2007, *A&A*, 464, 377
 Frinchauboy P. M., Majewski S. R., 2008, *AJ*, 136, 118
 González J. F., Lapasset E., 2000, *AJ*, 119, 2296
 González J. F., Veramendi M. E., Cowley C. R., 2014, *MNRAS*, 443, 1523
 Grenier S., Burnage R., Faraggiana R., Gerbaldi M., Delmas F., Gómez A. E., Sabas V., Sharif L., 1999, *A&AS*, 135, 503
 Grunhut J. H. et al., 2017, *MNRAS*, 465, 2432
 Grunhut J. H. et al., 2012, *MNRAS*, 426, 2208

- Heck A., Mathys G., Manfroid J., 1987, *Astronomy and Astrophysics Supplement Series*, 70, 33
- Hensberge H., van Rensbergen W., Blomme R., 1991, *A&A*, 249, 401
- Holdsworth D. L., Saio H., Bowman D. M., Kurtz D. W., Sefako R. R., Joyce M., Lambert T., Smalley B., 2018, *MNRAS*, 476, 601
- Horch E., van Altena W. F., Girard T. M., Franz O. G., López C. E., Timothy J. G., 2001, *AJ*, 121, 1597
- Howarth I. D. et al., 2007, *MNRAS*, 381, 433
- Hubrig S., Kurtz D. W., Bagnulo S., Szeifert T., Schöller M., Mathys G., Dziembowski W. A., 2004, *A&A*, 415, 661
- Hubrig S., North P., Schöller M., Mathys G., 2006, *Astronomische Nachrichten*, 327, 289
- Hubrig S., Szeifert T., Schöller M., Mathys G., Kurtz D. W., 2004, *A&A*, 415, 685
- Jaffe T. J., Barclay T., 2017, *tessgi/ticgen: v1.0.0*, Zenodo, doi:10.5281/zenodo.888217
- Jaschek C., Jaschek M., Gomez A., Grenier J. S., 1983, *A&A*, 127, 1
- Jenkins J. M. et al., 2016, in *Software and Cyberinfrastructure for Astronomy IV*. p. 99133E
- Kochukhov O., Bagnulo S., 2006, *A&A*, 450, 763
- Kochukhov O., Khan S., Shulyak D., 2005, *A&A*, 433, 671
- Kochukhov O., Rusomarov N., Valenti J. A., Stempels H. C., Snik F., Rodenhuis M., Piskunov N., 2015, *A&A*, 574, A79
- Kodaira K., 1969, *ApJ*, 157, L59
- Kodaira K., 1973, *A&A*, 26, 385
- Kopal Z., 1955, *Annales d'Astrophysique*, 18, 379
- Kreidl T. J., Kurtz D. W., Bus S. J., Kuschnig R., Birch P. B., Candy M. P., Weiss W. W., 1991, *MNRAS*, 250, 477
- Kurapati S. et al., 2017, *MNRAS*, 465, 2160
- Kurtz D. W., 1982, *MNRAS*, 200, 807
- Kurtz D. W., 1983, *MNRAS*, 205, 3
- Landstreet J. D., Bagnulo S., Andretta V., Fossati L., Mason E., Silaj J., Wade G. A., 2007, *A&A*, 470, 685
- Landstreet J. D., Bagnulo S., Fossati L., 2014, *A&A*, 572, A113
- Landstreet J. D., Mathys G., 2000, *A&A*, 359, 213
- Leone F., Catalano F. A., Manfre M., 1995, *A&A*, 294, 223
- Leto P. et al., 2018, *MNRAS*, 476, 562
- Lindgren L. et al., 1997, *A&A*, 323, L53
- Lomb N. R., 1976, *Ap&SS*, 39, 447
- Maitzen H. M., 1973, *Mitteilungen der Astronomischen Gesellschaft Hamburg*, 32, 252
- Maitzen H. M., 1976, *A&A*, 51, 223
- Maitzen H. M., 1976, *Mitteilungen der Astronomischen Gesellschaft Hamburg*, 38, 177
- Maitzen H. M., Breysacher J., Garnier R., Sterken C., Vogt N., 1974, *A&A*, 32, 21
- Maitzen H. M., Weiss W. W., Wood H. J., 1980, *A&A*, 81, 323
- Makarov V. V., Kaplan G. H., 2005, *AJ*, 129, 2420
- Manfroid J., Mathys G., 1985, *A&AS*, 59, 429
- Manfroid J., Mathys G., 1997, *A&A*, 320, 497
- Manfroid J., Renson P., 1981, *Information Bulletin on Variable Stars*, 2004
- Manfroid J., Renson P., 1983, *Information Bulletin on Variable Stars*, 2311
- Manfroid J., Renson P., 1994, *A&A*, 281, 73
- Marcolino W. L. F., Bouret J.-C., Sundqvist J. O., Walborn N. R., Fullerton A. W., Howarth I. D., Wade G. A., ud-Doula A., 2013, *MNRAS*, 431, 2253
- Marcolino W. L. F. et al., 2012, *MNRAS*, 422, 2314
- Martinez P., Kurtz D. W., 1990, *Information Bulletin on Variable Stars*, 3509
- Martinez P., Kurtz D. W., 1991, *Information Bulletin on Variable Stars*, 3553
- Martinez P., Kurtz D. W., 1994, *MNRAS*, 271, 118
- Martinez P., Kurtz D. W., Hoffman M. J. H., van Wyk F., 1995, *MNRAS*, 276, 1435
- Martinez P., Kurtz D. W., Kauffmann G. M., 1991, *MNRAS*, 250, 666
- Mathys G., 2017, *A&A*, 601, A14
- Mathys G., Hubrig S., 1997, *A&AS*, 124, 475
- Mathys G., Hubrig S., Landstreet J. D., Lanz T., Manfroid J., 1997, *A&AS*, 123, 353
- Medupe R., Kurtz D. W., Elkin V. G., Mguda Z., Mathys G., 2015, *MNRAS*, 446, 1347
- Mégessier C., 1974, *A&A*, 34, 53
- Mégessier C., 1975, *A&A*, 39, 263
- Michaud G., 1970, *ApJ*, 160, 641
- Montgomery M. H., Odonoghue D., 1999, *Delta Scuti Star Newsletter*, 13, 28
- Morel T. et al., 2015, in *Meynet G., Georgy C., Groh J., Stee P.*, eds, *IAU Symposium Vol. 307, New Windows on Massive Stars*. pp 342–347
- Morrison N. D., Wolff S. C., 1971, *Publications of the Astronomical Society of the Pacific*, 83, 474
- Munoz M., Wade G. A., Nazé Y., Bagnulo S., Puls J., 2018, *Contributions of the Astronomical Observatory Skalnaté Pleso*, 48, 149
- Nazé Y., Petit V., Rinbrand M., Cohen D., Owocki S., ud-Doula A., Wade G. A., 2014, *ApJS*, 215, 10
- Nazé Y., Walborn N. R., Morrell N., Wade G. A., Szymański M. K., 2015, *A&A*, 577, A107
- Neiner C., Mathis S., Alecian E., Emeriau C., Grunhut J., BinaM-IcS MiMeS Collaborations 2015, in *Nagendra K. N., Bagnulo S., Centeno R., Jesús Martínez González M.*, eds, *IAU Symposium Vol. 305, Polarimetry*. pp 61–66
- North P., 1984, *A&AS*, 55, 259
- North P., 1987, *A&AS*, 69, 371
- North P., Brown D. N., Landstreet J. D., 1992, *A&A*, 258, 389
- North P., Burnet M., 1991, *Information Bulletin on Variable Stars*, 3635
- North P., Rufener F., Bartholdi P., 1982, *Information Bulletin on Variable Stars*, 2103
- Oksala M. E., Grunhut J. H., Kraus M., Borges Fernandes M., Neiner C., Condori C. A. H., Campagnolo J. C. N., Souza T. B., 2015, *A&A*, 578, A112
- Oksala M. E. et al., 2015, *MNRAS*, 451, 2015
- Owocki S. P., ud-Doula A., Sundqvist J. O., Petit V., Cohen D. H., Townsend R. H. D., 2016, *MNRAS*, 462, 3830
- Paunzen E., Hensberge H., Maitzen H. M., Netopil M., Triglio C., Fossati L., Heiter U., Pranka M., 2011, *A&A*, 525, A16
- Paunzen E., Maitzen H. M., 1998, *A&AS*, 133, 1
- Pedersen M. G. et al., 2019, *ApJ*, 872, L9
- Petit V. et al., 2013, *MNRAS*, 429, 398
- Renson P., 1978, *Information Bulletin on Variable Stars*, 1391
- Renson P., 1979, *A&A*, 77, 366
- Renson P., Manfroid J., 2009, *A&A*, 498, 961
- Ricker G. R. et al., 2015, *Journal of Astronomical Telescopes, Instruments, and Systems*, 1, 014003
- Rivinius T., Townsend R. H. D., Kochukhov O., Štefl S., Baade D., Barrera L., Szeifert T., 2013, *MNRAS*, 429, 177
- Ryabchikova T., Sachkov M., Kochukhov O., Lyashko D., 2007, *A&A*, 473, 907
- Samus' N. N., Kazarovets E. V., Durlevich O. V., Kireeva N. N., Pastukhova E. N., 2017, *Astronomy Reports*, 61, 80
- Sanz-Forcada J., Franciosini E., Pallavicini R., 2004, *A&A*, 421, 715
- Scargle J. D., 1982, *ApJ*, 263, 835
- Schöller M., Correia S., Hubrig S., Kurtz D. W., 2012, *A&A*, 545, A38
- Schwarzenberg-Czerny A., 2003, in *Sterken C.*, ed., *Astronomical Society of the Pacific Conference Series Vol. 292, Interplay of*

- Periodic, Cyclic and Stochastic Variability in Selected Areas of the H-R Diagram. p. 383
- Seabold S., Perktold J., 2010, in Proceedings of the 9th Python in Science Conference. p. 61
- Sikora J., Wade G. A., Power J., Neiner C., 2019, MNRAS, 483, 2300
- Silvester J., Kochukhov O., Rusomarov N., Wade G. A., 2017, MNRAS, 471, 962
- Snowden M. S., 1975, PASP, 87, 721
- Stahl O. et al., 1996, A&A, 312, 539
- Stassun K. G. et al., 2018, AJ, 156, 102
- Stibbs D. W. N., 1950, MNRAS, 110, 395
- Struve O., 1952, Annales d'Astrophysique, 15, 157
- Szewczuk W., Daszyńska-Daszkiewicz J., 2015, MNRAS, 450, 1585
- Townsend R. H. D., 2002, MNRAS, 330, 855
- Townsend R. H. D., 2008, MNRAS, 389, 559
- Townsend R. H. D., Owocki S. P., 2005, MNRAS, 357, 251
- Townsend R. H. D. et al., 2013, ApJ, 769, 33
- ud-Doula A., Owocki S. P., 2002, ApJ, 576, 413
- ud-Doula A., Owocki S. P., Townsend R. H. D., 2009, MNRAS, 392, 1022
- ud-Doula A., Sundqvist J. O., Owocki S. P., Petit V., Townsend R. H. D., 2013, MNRAS, 428, 2723
- van Dijk W., Kerssies A., Hammerschlag-Hensberge G., Wesseliuss P. R., 1978, A&A, 66, 187
- van Heerden P., Martinez P., Kilkenny D., 2012, MNRAS, 426, 969
- Wade G. A. et al., 2014, in Petit P., Jardine M., Spruit H. C., eds, IAU Symposium Vol. 302, Magnetic Fields throughout Stellar Evolution. pp 265–269
- Wade G. A. et al., 2011, MNRAS, 416, 3160
- Waelkens C., Aerts C., Kestens E., Grenon M., Eyer L., 1998, A&A, 330, 215
- Waelkens C., Rufener F., 1985, A&A, 152, 6
- Warhurst P. M., 2004, Baltic Astronomy, 13, 597
- Wenger M. et al., 2000, A&AS, 143, 9
- Wolf S. C., 1981, ApJ, 244, 221
- Yakunin I. et al., 2015, MNRAS, 447, 1418

APPENDIX A: PHASED LIGHT CURVES

In this section, we present phase folded light curves for each star showing rotational modulation (with overlaid binned light curves using 20 phase bins over the full rotational cycle).

This paper has been typeset from a $\text{\TeX}/\text{\LaTeX}$ file prepared by the author.

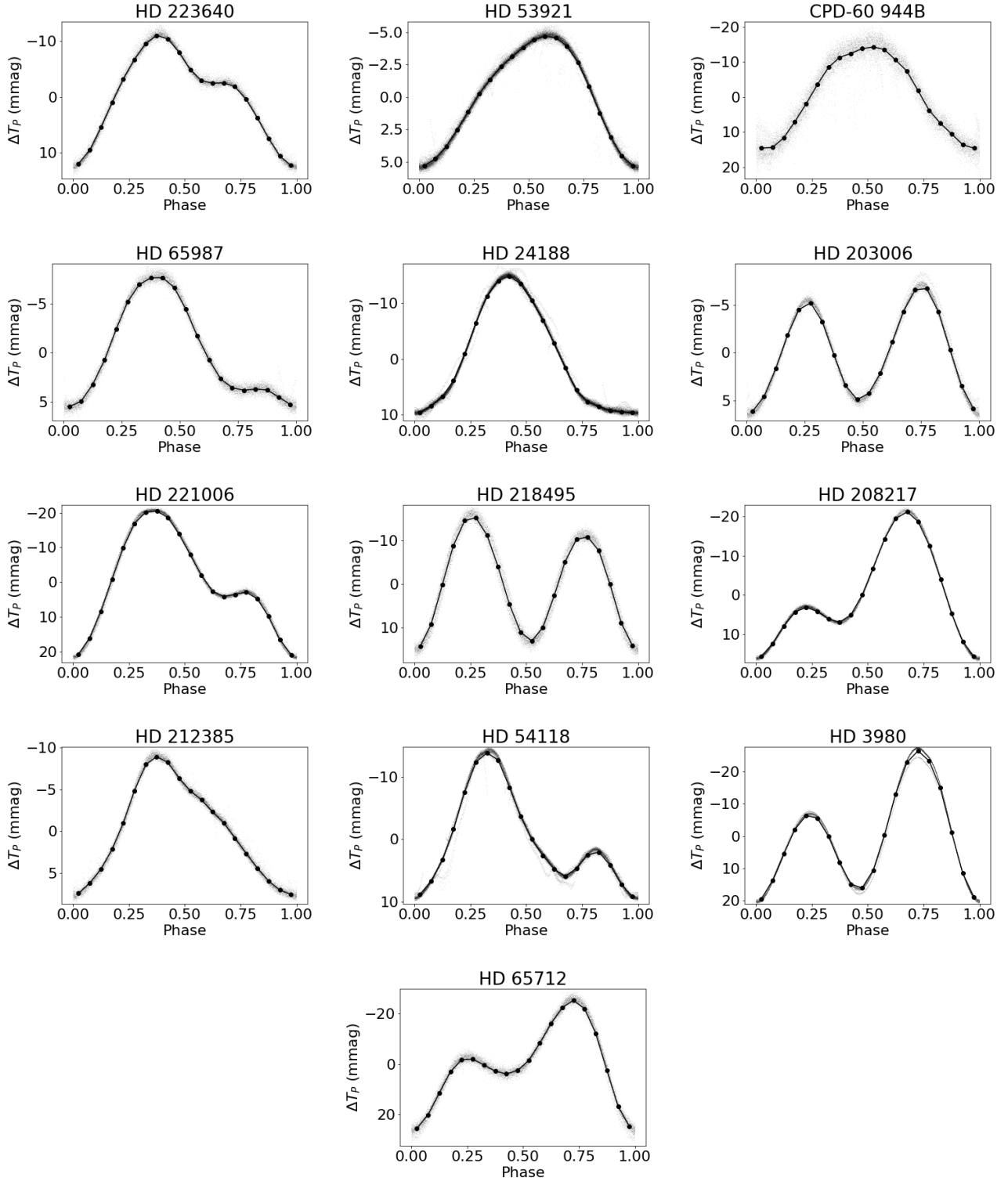


Figure A2. Phase folded light curves (with phase 0 corresponding to minimum light) for the thirteen stars showing potential rotational modulation. The light grey points correspond to individual measurements, and the larger black points connected by a line correspond to binned data (with bins of 0.05 in phase). For some stars, we see streaks of outliers; these are due to artefacts which could not be completely detrended. We find that the light curves have diverse morphologies, with at least nine out of the thirteen showing signs of double-wave variations, and all of them having an asymmetric profile.